NEW RESULTS OF CdS/Cu$_2$S SOLAR CELL RESEARCH

K. W. Boer

Institute of Energy Conversion
University of Delaware
Newark, Delaware 19711, USA

Sep 74   16 p.

SUMMARY

The most significant results of the Delaware team are summarized. The CdS/Cu$_2$S band model is further developed, and the space charge region in CdS is analyzed. Field enhanced recombination seems to limit the field near the interface. This and possibly other field effects force continuity of both quasi-Fermi levels through the interface. The Cu$_2$S predominantly determines the current; the CdS seems to determine the open circuit voltage behavior of the cell.

INTRODUCTION

CdS/Cu$_2$S solar cells are being investigated by a team of researchers at the University of Delaware. The most significant results obtained so far relate to a better understanding of the cell conversion mechanism, the cell structure, an improvement of the production yield and an increase of the life expectancy, and are published in a sequence of reports (1) to the National Science Foundation, which sponsors major parts of the research.

The cells have a 55 cm^2 CdS/Cu$_2$S surface area and are covered with photo-etched gold-plated copper grids of 4 X 24, 8 X 8, 6 X 6 or 4 X 4 lines per cm, covered with a thin Mylar film. Wider grids show higher currents substantially beyond expectation because of increased optical transparency. Spacing is limited by the Cu$_2$S sheet resistance ρ which, over a wide range of short circuit currents j_{sc}, is related as $j_{sc} \sim \rho^{\frac{1}{2}}$. For cells of 4% conversion efficiency, a grid spacing of 6 X 6 is nearly optimum (1)(2).

The cells can be made reproducibly in the 3-4% efficiency range by evaporation of CdS onto a well cleaned zinc-plated copper foil and by ion exchange of a 0.2 μm thick surface layer into Cu$_2$S after a short HCl etch, as long as care is taken to avoid the presence of divalent copper ions in the ion exchange bath. Post deposition treatments in air and later in vacuum are critical to achieve acceptable short circuit currents and fill factors (3).

Marked enhancements of efficiencies after additional copper deposition and heat treatments, as reported by Bogus (4), have been substantiated (3). All acceptable cells show exclusively chalcocite structure and Cu$_2$S composition of the top layer within the experimental error of the Auger-analysis (3). The lattice constant d(600) of Cu$_2$S was redetermined (5) using Moiré fringes on a CdS host lattice for reference and a new

value of 1.996 ± 0.003, 1.06% larger than the previously established value, was established (6). A reversible bulk allotropic transition of chalcocite in contact with CdS at $110^{\circ} \pm 5^{\circ}C$ is observed (7).

Life testing and accelerated life testing substantiate life expectancies in excess of 15 years for actual rooftop deployments. No degradation is observed on an array of 104 cells deployed in ultra-pure N_2 on Solar One within one year (8). Extrapolated life expectancies of single cells for rooftop conditions vary, dependent on cell preparation. The best currently measured life expectancy (at $56^{\circ}C$ and in N_2) is approximately 100 years (3)(9).

Long term degradation in N_2 seems to be associated with diffusion of copper. Published data on diffusion rates are compatible with this hypothesis (10)(11).

Degradation in the presence of oxygen and water vapor is at least partially reversible after a 10-20 hr heat treatment in H_2 at $130^{\circ}C$ and consequent cell deposition in N_2 for several weeks (3).

The improved understanding of the cell centered around an analysis of the I-V characteristics, which can be described near room temperature by a parallel circuit of two diodes with a simple shunt and series resistance* (Fig. 1):

$$I' = I_{01}[\exp(\frac{eV'}{A_1 kT}) - 1] + I_{02}[\exp(\frac{eV'}{A_2 kT}) - 1] - I_L \qquad (1)$$

This picture is in approximate agreement with a band model first suggested by Shiozawa (12) and shown in Fig. 2; however, it is modified by a specific level R at 0.45 eV above the valence band of Cu_2S (13)(14). One diode seems to represent recombination at this level with an activation energy for I_{01} of 0.45 eV (in the light) and $A_1 \simeq 2$. This diode dominates at "low" forward voltages.** The other diode dominates at high voltages and seems to represent back diffusion over the barrier with an activation energy for I_{02} of approximately barrier height (1.1 eV) and $A_2 \simeq 1$ in agreement with a simple leakage current theory (2)(15).

This model seems to be capable of explaining major features of the barrier. However, a more detailed recent analysis indicates that modifications are necessary. A summary of this analysis is the main topic of this paper.

BAND MODEL OF THE CdS/Cu_2S HETEROJUNCTION

---

* I' and V' are reduced parameters excluding series and shunt resistances.
**The boundary between the "low" and "high" voltage range increases with increasing light intensity and changes with other cell parameters. At AM1, $20^{\circ}C$, it is slightly below V_{oc} (open circuit voltage).

The model given in Fig. 2 needs to be refined by space charge considerations causing band bending and fields, which in turn may interact with the space charge via field induced carrier transitions. That such interaction is indeed probable can best be seen by separating CdS and Cu_2S and illuminating both slabs. In both slabs carrier and minority carrier densities will then increase to an extent given by excitation and recombination; two quasi-Fermi levels will split from the Fermi-level in each material independent from each other.

When CdS and Cu_2S are then brought together into intimate contact, this independence disappears. This can best be seen by analyzing the open circuit case.

Open Circuit Conditions

Without Light. By some initial charge transport between CdS and Cu_2S after joining the two materials, they are connected in such a way that the Fermi-level adjoins at the interface (Fig. 2). In steady state the density of carriers* at both sides of the interface is given that no current flows

$$j = j_n = j_p = 0. \tag{2}$$

For electrons, that means that Richardson emission from the Cu_2S is exactly compensated by back diffusion of electrons from the CdS into and over the barrier.

Inside each material, a diffusion potential near the barrier compensates exactly for carrier diffusion.

$$j_n = e\mu nF - \mu kT \frac{dn}{dx} = 0 \tag{3}$$

For reason of an estimated hole density in excess of 10^{18} cm^{-3}, the influence of space charge effects near the interface, on carrier transport, is usually neglected in Cu_2S.

In CdS, however, the space charge near the barrier seems to determine the diode behavior to a major extent. With a currently accepted conduction band interconnect at 0.85 eV above E_v (Cu_2S), and for properly conductive CdS (surplus Cd) with E_c (CdS) - $E_F \approx 0.2$ eV in the CdS bulk, a diffusion potential of 0.65 volt is needed.

Capacitance measurements of small segments (.04 cm^2) of these solar cells have shown two linear ranges in the $1/C^2$ vs. V plot. This indicates space charge distribution as given in Fig. 3, resulting in a very sharp increase (<100Å) of the field to about 20 kV/cm at about 0.3μm from the interface and then a much

---

*A careful accounting of the density at each energy state and transition probability at each state through the interface is necessary.

3

less pronounced further increase of the field (3) (in the scale of Fig. 2 this looks like a kink and a straight line rise of the potential). The field distribution has nearly step - or domain (16) - characters, indicating some field limiting process near 0.65 Volt/0.3µm ≈ 20kV/cm (treatment 70 min at 150°C).

With Light. Again, both materials are connected in such a way that the quasi-Fermi levels connect. However, since their separation in the bulk is fixed by independent means, a connection of both quasi-Fermi levels needs an additional mechanism of matching this separation at the interface and joining properly from both materials; such mechanism involves probably recombination at the interface. However, quasi-Fermi levels cannot bend in an arbitrary fashion since their slope is connected with the net current.

$$j_n = e\mu_n n F - \mu_n k T \frac{dn}{dx} = \frac{\sigma_n}{e} \frac{dE_{Fn}}{dx} \qquad (4)$$

and similarly for the hole current.

For open circuit conditions, one therefore obtains from

$$j = j_n + j_p = 0 \qquad (2a)$$

the condition (15)

$$\sigma_n \frac{dE_{Fn}}{dx} = -\sigma_p \frac{dE_{Fp}}{dx}. \qquad (5)$$

Hence, the quasi-Fermi level for holes must have an opposite slope to the quasi-Fermi level for electrons, and the relative slopes are proportionate to the inverse of the relative conductivities (Fig. 4).

This indicates that the interconnection of bands at a heterojunction under light is a severe restraint which forces continuous current adjustment at and near the interface (j_n and j_p are not zero) via generation and recombination. It is indicated that field-induced redistribution of carriers near the interface could provide the necessary modification of the space charge in such a way that via such feedback Equation 5 could be satisfied.

Experimentally it is observed (17) that the space charge region shrinks with light and the difference in charge densities decreases somewhat (Fig. 3); however, it indicates a similar domain-like field distribution as in the dark, possibly with a somewhat lower field. The domain is also thinner, the diffusion voltage is smaller (reduced by approximately the open circuit voltage - see Fig. 4).

Again, the field in the domain can only be of the order of 20 kV/cm. Such fields are too small to explain marked tunneling currents in the slab (18); however, they could cause field enhanced ionization (19) from levels distributed in a 0.2 µm thick slab in which the field adjustment seems to take place.

The observed behavior has great similarity with field en-

hanced quenching, an effect well-known and studied in CdS (20)
(21). Field quenching is easily able to adjust the space charge
over a wide range of densities, including all values shown in
Fig. 3, since centers on which such quenching operates are known
to exist in CdS in excess of $3 \times 10^{17} cm^{-3}$. Such field quenching
also limits conveniently the field as can best be seen from the
field of direction (21) for solutions of the Poisson and trans-
port equations, as shown in Fig. 5, which depicts a possible
solution (curved arrow) between singular points II and I, having
the domain character as indicated in the experiment. In the
case shown in Fig. 5, the field near the interface in CdS cannot
exceed the field at the point II which usually lies in the 15 to
50 kV/cm range (20).

Copper Diffusion Consideration

It is known that the density of Coulomb-attractive centers
can change markedly the field enhanced ionization probability
when the density of these centers becomes large enough so that
their Coulomb tunnels overlap and reduce connecting saddlepoints
by more than kT (19). This is the case at density already above
$10^{15} cm^{-3}$.

When such considerable overlap exists, the quasi-neutrality
curve $n_1(x)$ in Fig. 5, and hence the critical fields at the
singular point II (F_{II}), can change substantially. Such changes
have directly been observed (22) for CdS single crystals doped
with different densities of silver (Fig. 6).

Copper as dopant behaves very similarly to silver and is
known to produce in CdS a Coulomb-attractive center for holes
when substituting a Cd lattice ion. It can be incorporated into
CdS well in excess of $10^{15} cm^{-3}$ before saturation; hence a behav-
ior similar to Ag-doped CdS is expected.

This may present an alternative possibility to explain the
effects of copper diffusion in CdS (10): With increasing center
density, the high field limit F_{II} decreases, hence the thickness
of the slab (= thickness of high-field domain) must increase, as
observed. A careful analysis of the diffusion kinetics is nec-
essary before conclusions can be reached about the possible
validity of the proposed model. If substantiated, this model
could help to explain the differences in life expectancy for
differently prepared (doped) CdS/Cu$_2$S solar cells.

Light Induced Current

It is generally accepted that the major fraction of the
photovoltaic current (short circuit current) is an electron
current generated in Cu$_2$S. This conclusion is based primarily
on the optical absorption of the Cu$_2$S, its optimum thickness,
and front- vs. back-wall experiments with thin-film cells.

Observed short circuit current densities close to 30 mA/cm^2
at 100 mW/cm^2 AM1 irradiation indicate collection efficiencies
at the interface in excess of 50% for a flat surface; that is,
assuming that every photon with an energy larger than the gap
absorbed in the Cu$_2$S produces an electron/hole pair, and more

than 50% of these electrons cross the interface before they have time to recombine.

This provides an interesting base for some estimates for CdS/Cu$_2$S cells in which such high current densities are observed:

1. Recombination at the outer surface must be negligible since only under these conditions more than 50% of generated carriers can leave a slab through one surface (23). This may indicate the existence of a potential barrier at the surface of such cells with high current densities.

2. It is unlikely that a drift field across the entire Cu$_2$S slab exists which provides such efficient carrier transport. From a simple drift current estimate one concludes that the nF product would have to exceed* 10^{16} V/cm^4. For $n \leq 10^{12}$cm^{-3} (see below), it follows that $F \geq 10^4$ V/cm, or across the slab of 2000 Å thickness a potential drop of 0.2 eV must be sustained. For a highly degenerated Cu$_2$S, this is too high. It is questionable that a properly graded variation of the degeneration towards the surface can be achieved. Hence it is suggested that carrier diffusion, rather than drift, accounts for the current within the Cu$_2$S.

3. The diffusion length will be of the order of the thickness of the Cu$_2$S slab, which in turn must be of the order of 1/K (K = "average" absorption constant at $5,000 < \lambda < 10,000$Å). With an experimentally observed "optimum" slab thickness of 2,000Å, one estimates a minority carrier lifetime of $\tau_n \sim 10^{-10}$ sec. With a generation rate (AM1, E > 1.2 eV) of $\approx 10^{22}$/cm^{3}s, one concludes that a bulk density of $n \approx 10^{12}$cm^{-3} is expected.

4. Such minority carrier density requires a quasi-Fermi level at $E_c - E_{Fn} \approx 0.4$ eV in the Cu$_2$S bulk. Richardson emission of electrons into CdS requires a density of approximately 10^{10}cm^{-3} at the interface and yields a proper magnitude of the diffusion current sustaining the Richardson emission:

$$j_n/\mu_n kT \approx \Delta n/\Delta X \approx 10^{18}\text{cm}^{-4} \text{ for } n_{bulk} \approx 10^{11}\text{cm}^{-3},$$

indicating that the value estimated in the previous section is about correct, and probably an upper bound. The quasi-Fermi level at the interface, however, has to be not more than 0.52 eV from the conduction band of Cu$_2$S in order to provide the observed current.

5. In open circuit conditions the tilting of the electron quasi-Fermi level from the bulk to the interface is

*assuming $\mu_n \approx 20$ cm^2/Vs

6

essentially* eliminated, hence here $E_c - E_{F_n}$ must be smaller than 0.52 eV and probably close to 0.45 eV (corresponding to $n \simeq 10^{11} cm^{-3}$).

Consideration of Recombination in CdS

If the above assumptions are correct and the electron quasi-Fermi level would stay horizontally in CdS for open circuit conditions, one would expect an open circuit voltage of Cu_2S gap minus 0.45 eV, i.e. of 0.75 Volt. This is substantially above the highest currently observed open circuit voltage (0.53 Volt) at AM1, 25°C.

It is necessary to assume recombination at the interface if a downwards slope of E_{F_n} in CdS towards the interface is required (see Fig. 4). Such slope would indeed reduce the open circuit voltage below the theoretical limit of 0.75 Volt.

However, it is improbable that a reduction of more than 0.2 eV is possible for the majority quasi-Fermi level as long as Equation 5 holds. Field induced charge transport through the interface must be carefully analyzed to account for additional recombination. Such analysis could be the key for further cell improvement above 10% conversion efficiency.

SUMMARY AND CONCLUSIONS

In a CdS/Cu_2S solar cell, the Cu_2S provides the major fraction of the photovoltaic carriers and is responsible for the short circuit current. In efficient cells more than 50% of the photons absorbed in the Cu_2S produce electrons which contribute to the current.

The CdS seems to determine the recombination responsible for limiting the open circuit voltage. Forced recombination via field effects is probably a major effect at heterojunctions to permit continuity of both quasi-Fermi levels at the interface.

Field quenching influences the distribution of trapped charges, and evidence is obtained that such mechanism may limit the field near the interface in CdS.

A band model is given which describes part of the observed behavior. Further studies of field enhanced charge transitions through the interface and a critical reevaluation of currently accepted assumptions are necessary before further conclusions are reached. Presently, a considerable improvement of cell performance beyond current achievements seems possible.

Acknowledgement

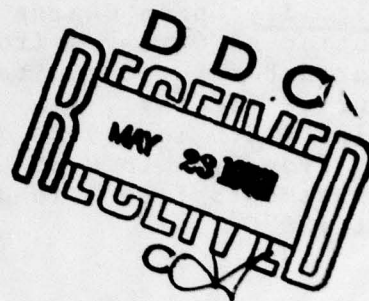It is a great pleasure to acknowledge the many contributions

---

*not totally because of Equation 5, however, it is a good approximation because $\sigma_p \gg \sigma_n$.

of the members of the research team. Special thanks are due to Drs. A. Rothwarf and H. C. Hadley, Jr., and to Mr. J. E. Phillips for many discussions, and to Dr. V. J. Singh for communicating the results of his capacitance measurements (Fig. 3).

REFERENCES

1. Progress and Technical Reports NSF/RANN/SE/GI-34872, 1973-4.

2. K. W. Böer et al., 10th IEEE Photovoltaic Specialists Conference, pp. 77 ff (1973).

3. Semi-annual Progress Report NSF/RANN/SE/GI-34872/PR74/2.

4. K. Bogus and S. Mattes, 9th IEEE Photovoltaic Specialists Conference, pp. 106 (1972).

5. I. G. Greenfield and W. F. Tseng, Phys.Stat.Sol. (in print).

6. W. R. Cook, Jr., L. R. Shiozawa and F. Augustine, J.Appl. Phys. 41, 3058 (1970).

7. Quarterly Progress Report NSF/RANN/SE/GI-34872/PR74/1.

8. K. W. Böer, Proceedings of the International Conference on Photovoltaic Power Generation, Hamburg (1974).

9. H. M. Windawi, personal communication, Technical Report in preparation.

10. G. A. Sullivan, Phys. Rev. 184, 796 (1969).

11. C. E. Birchenall and T. L. Lu, Technical Report NSF/RANN/SE/-GI-34872/TR73/7.

12. L. R. Shiozawa, G. A. Sullivan, F. Augustine, T. M. Smith III and W. R. Cook, Jr., Final Report AF 33(615)-5224 (1969).

13. K. W. Böer, Final Report NASA JPL, No. 952666, Oct. 1970.

14. A. Fahrenbruch, Ph.D. Thesis, Stanford University (1973).

15. K. W. Böer and J. Phillips, 9th IEEE Photovoltaic Specialists Conference, pp. 125 (1972).

16. K. W. Böer, Proc. III International Conference on Photoconductivity, Pergamon Press, pp. 75 ff (1971).

17. V. J. Singh, personal communication.

18. G. A. Dussel, K. W. Böer and R. J. Stirn, Phys. Rev. 7B, 1443 (1973).

19. G. A. Dussel and K. W. Böer, Phys. Stat. Sol. 39, 375 (1970).

20. G. A. Dussel and K. W. Böer, Phys. Stat. Sol. 39, 391 (1970).

21. K. W. Böer, G. Döhler, G. A. Dussel and P. Voss, Phys. Rev. 169, 700 (1968).

22. H. Hadley and K. W. Böer, Phys. Stat. Sol. (a) 11, K145 (1972).

23. A. Rothwarf in (3) and (7).

Fig. 1: Equivalent Circuit of the CdS/Cu_2S Cell

Fig. 2: Band Model of a CdS/Cu_2S Heterojunction (energies to scale; no light); D_1:Diode 1 leakage current; D_2: Diode 2 leakage current; M_1 and M_2: Metals

Fig. 3: Space Charge Distribution as Obtained from Measured Barrier Capacitance Curves ($1/C^2$ vs. V). The slab width increases linearly from 0.25 to 0.65 µm with treatments from 1 to 3 hrs at 150^oC.

Fig. 4: Barrier Region with Optical Excitation Quasi-Fermi Levels near the Interface are Drawn Schematically with Slope Ratios Not to Scale.

Fig. 5: Field of Direction. $n_1(F)$:Quasi-Neutrality Curve ($\rho(F) \equiv 0$) and $n_2(F)$:Drift-Current Curve ($nF \equiv j/e\mu$). Straight Arrows Symbolize Quadrants of Possible Directions.

Fig. 6: Field-Dependent Carrier Density. Decrease Caused by Field Quenching. Doped with Ag to Given ppm and Partially Compensated with Al.

E_c

D_2

D_1

R

E_F

E_V

M_1

M_2

Cu_2S

CdS

11